A study of thermal nonequilibrium effects in low-pressure wet-steam turbines using a blade-to-blade time-marching technique

M. Moheban* and J. B. Young†

A theoretical analysis of the wet-steam flow in the low pressure cylinder of a 500 MW steam turbine using a blade-to-blade time-marching computer program is described. The calculating method can compute most types of wet-steam flow found in LP turbines, including those involving both primary and secondary nucleations in transonic and supersonic blading with shock waves. In particular, condensing flows in highly staggered rotor tip sections can be computed without difficulty. Extensive results are presented showing the effect of departures from thermal equilibrium on the blade surface pressure and velocity distributions, the blade outlet relative flow angle, the mass flow coefficient and the thermodynamic loss coefficient. On the basis of the analysis, recommendations are made concerning the application of nonequilibrium wet-steam theory to steam turbine design.

Keywords: *two-phase flow, air-lift pumps*

Most steam turbines built for large scale electricity generation operate with several stages in the two-phase, wet-steam region. In those turbines associated with fossil fuelled power stations or gas cooled nuclear reactors, the wetness is confined to the last few stages of the low pressure cylinder; but in turbines operating with water cooled reactors, the steam in the high pressure cylinder is also wet.

From the standpoint of the turbine designer, the effects of wetness are twofold. First, turbine stages passing wet steam incur a loss over and above that associated with their dry steam operation. Second, there is the probability of blade erosion (and possible failure) due to the continual bombardment of the blades by the water droplets.

The magnitude of the wetness loss is still a matter for conjecture, although it is known that it can achieve an importance in the final stage of a low pressure turbine comparable to that of the profile and secondary losses combined. Furthermore, measurements in high pressure turbines[1] have indicated that it can play an even more dominating role in nuclear sets. However, despite the fundamental nature of the wetness loss, most turbine manufacturers still employ unchanged the Baumann empirical correlation[2] and have made little attempt to grapple with a problem which research has, admittedly, shown to be extremely complex.

Wetness and nonequilibrium effects in steam turbines can conveniently be subdivided into two categories. Category one comprises those effects which might be termed *direct wetness losses*, ie those phenomena which are responsible for the production of entropy as a direct consequence of the presence of water. According to Gyarmathy[3], these include the thermodynamic loss, droplet drag loss, deposition loss, braking and centrifuging losses, etc. Category two, on the other hand, is involved with the indirect effects of wetness. These are aerodynamic in origin, but are brought about by changes in the flow distribution due directly to departures of the wet steam from thermal and inertial equilibrium. Category two effects do not necessarily result in reduced turbine efficiency and, indeed, it is possible that departures from equilibrium might result in improved performance of the blading.

In order to quantify the effects of thermal nonequilibrium on the flow distribution in turbines, a number of computational methods have recently appeared in the literature dealing specifically with the application of wet-steam theory to the calculation of flows in turbomachinery: in particular, a throughflow calculation method based on the streamline curvature technique[4,5], and the calculation of blade-to-blade flows by time-marching methods[6–8].

This paper also deals with nonequilibrium flows in the blade-to-blade plane. The basic solution technique has already been described in a previous publication[9], but the computer program has now been extended and is capable of computing most types of flows found in wet-steam turbines, including those involving secondary nucleation. A large number of calculations have been performed on a variety of radically different blade profiles from the low pressure cylinder of a 500 MW turbine-generator set. In the light of these results, it is possible to make a valid assessment of the potential improvements accruing from nonequilibrium rather than equilibrium design methods.

* University of London, Imperial College, Exhibition Road, London SW7
† Whittle Laboratory, University of Cambridge, Trumpington Street, Cambridge
Manuscript received 18 October 1984 and accepted for publication 7 March 1985

 0142–727X/85/040269–10$3.00

Theory and computational method

The results presented below were computed using a technique devised by the authors for calculating steady, inviscid, two-dimensional, nonequilibrium, wet-steam flows in turbine cascades. The solution method is fully described in Ref 9 and will not be repeated here. The following is just a brief outline of the procedure.

The basic conservation equations of continuity, momentum and energy for a two-phase flow of wet steam are solved in conjunction with the nucleation and droplet growth equations by a time-marching method modelled on the single-phase technique of Denton[10]. The equations are discretized on a computational grid of non-overlapping trapeziums formed by the intersection of straight quasi-orthogonals (in the circumferential direction) and curved quasi-streamlines (in the streamwise direction). With the assumption of zero interphase velocity slip between droplets and vapour, the continuity and momentum equations are identical to those for single-phase flow and their treatment parallels exactly the method described in Ref 10. In particular, the same techniques are used to ensure numerical stability. When dealing with the nucleation and droplet growth processes, however, a novel procedure is employed whereby these equations are combined with the energy equation, resulting in expressions for the changes in supercooling and wetness fraction along true (as opposed to quasi-) streamlines. By using an analytically integrated version of the supercooling equation, the intrinsic mathematical stiffness of the governing equations is removed and computational stability and efficiency greatly improved.

Because of the assumption of zero interphase velocity slip (ie complete inertial equilibrium), the computer program can only furnish information on departures from thermal equilibrium. Despite this restriction, the calculations presented below prove it to be very versatile and capable of computing most types of two-dimensional steam flow found in turbines. In particular it can deal with both primary and secondary nucleations, together with non-nucleating flows where the steam is already wet at cascade inlet.

In calculating the nucleation and droplet growth rates, 'classical' theories have been adopted as described in Ref. 9. It has also been assumed that, for calculation purposes, the nucleation process can be characterized by a single, average droplet radius representing the complete spectrum of droplet sizes. This approximation is commonplace in wet-steam work and leads to large reductions in cpu requirements. It is justifiable because the results of the calculations agree closely with those of more elaborate procedures and also with experimental data. Indeed, results computed by the authors' program have been compared with the available experimental measurements on condensation 'shocks' in converging–diverging nozzles, and good agreement was obtained over a wide range of conditions[9]. It should be noted, however, that implicit in the calculation procedure for nucleation is the assumption that condensate nuclei form in laminar steady flow. Although this is a good approximation for nucleation in laboratory nozzles, it is now thought that high levels of turbulence in the blade wakes and even in the mainstream may cause a change in the characteristics of nucleation in turbines. No attempt has been made to include these effects in the present calculations as the underlying physical phenomena are not yet fully understood.

One drawback of the time-marching solution procedure as presently implemented is the necessity of adding a 'fluid cusp' to the leading edge of the blade in order to prevent numerical flow reversal in the vicinity of the stagnation point. This is a common remedy for a difficult problem associated with many time-marching methods, but is thought to affect the solution only locally. On the credit side is the undoubtedly beneficial effect in minimizing losses in total pressure due to numerical inaccuracy in a region where the velocity gradients are very high.

The computation efficiency of the method is excellent in comparison with most wet-steam calculation procedures and has been further enhanced by a 'multigrid' technique almost identical to that described in Ref 10. A typical solution on a 60×10 grid takes about four minutes on an IBM 3081, which is approximately double the requirement for an equivalent single-phase superheated solution.

Cascade performance parameters

Two-dimensional nonequilibrium calculations can sumply information on a number of different aspects of blade performance, including:

(1) blade surface pressure and velocity distributions;
(2) blade outlet flow velocities and angles;
(3) circumferential variation of flow properties at cascade outlet;
(4) the mass flow coefficient, ϕ;
(5) the thermodynamic loss coefficient, ξ_T;
(6) the average droplet radius formed as a result of

Notation

c_p Isobaric specific heat capacity
h Specific enthalpy
p Pressure
R Specific gas constant
r Droplet radius
s Specific entropy
T Temperature
V Velocity
y Wetness fraction
β Relative flow angle
ΔT Supercooling
ϕ Mass flow coefficient
ξ_T Thermodynamic loss coefficient
ρ Density

Subscripts

e Equilibrium
ex Blade exit
g Vapour phase
l Liquid phase
ne Nonequilibrium
o Inlet stagnation condition
s Saturation condition
T Thermodynamic

nucleation within the blade passage;
(7) the deviation of the wetness fraction from its equilibrium value at any point in the flowfield.

The blade surface pressure distribution is of obvious importance to the turbine designer. Not only does it confirm that the desired stage loading is attainable, but it also furnishes information concerning boundary layer development and possible separation. Due to the lack of experimental data on blade surface pressure distributions in condensing flows, all the nonequilibrium calculations presented below are compared with calculations assuming equilibrium flow across the same pressure ratio. The latter were carried out using an identical equation of state for the vapour phase. This type of comparison is very instructive as it gives the designer an immediate appreciation of the possible advantages, if any, of undertaking a blade design using nonequilibrium methods.

The importance of information concerning blade exit flow velocities and angles is self-evident as the flow incidence onto the following blade row can be crucial in ensuring good performance, especially for final stage rotor tip sections. Circumferential variations in exit flow properties are also of interest when justifying axisymmetric throughflow calculations.

The tendency of a cascade to pass a higher mass flowrate with increasing departure from thermal equilibrium is well known and the mass flow coefficient ϕ is defined by

$$\phi = \frac{\text{actual mass flowrate}}{\text{equilibrium mass flowrate}} \tag{1}$$

where the equilibrium mass flowrate is that calculated by assuming the steam to expand in thermodynamic equilibrium across the same pressure ratio. As shown below, the mass flow coefficient is a strong function of droplet radius and wetness fraction.

In a real LP turbine the mass flowrate is, of course, constant throughout the machine (in the absence of bleed flows) and is effectively fixed by the first stage where the steam is invariably superheated. Departures from equilibrium therefore manifest themselves as variations in the pressure distribution throughout the turbine and these can only be estimated satisfactorily using a nonequilibrium throughflow procedure such as that described in Refs 4 and 5. Even without such sophistication, however, mass flow coefficients are a valuable indication of the likely changes in pressure level throughout the machine and can even be incorporated into standard equilibrium throughflow programs as pseudo-nonequilibrium correction factors.

The thermodynamic wetness loss is a direct consequence of the irreversible heat and mass transfer which accompanies the phase change during condensation. This can be calculated by the procedure described in Ref 9 and the *thermodynamic loss coefficient* ξ_T for the blade row is defined by

$$\xi_T = \frac{T_s \Delta s_T}{V_{ex}^2/2}$$

where Δs_T is the thermodynamic entropy increase across the blade row and T_s and V_{ex} are the saturation temperature and relative flow velocity at blade exit respectively. All quantities are mass-averaged across the pitch.

The thermodynamic wetness loss is only one component of the overall wetness loss, but the other components cannot be calculated from the type of blade-to-blade analysis described here. However, they are known to be strong functions of the prevailing fog droplet size, a parameter which emerges directly from the nucleation calculations. The mean fog droplet radius is also of interest because it plays a major role in controlling the magnitude of departures from equilibrium in succeeding blade rows.

Order of magnitude calculations

Before discussing the full two-dimensional cascade solutions, it is instructive to consider some simple order of magnitude calculations which give considerable insight into the possible effects of departures from equilibrium. Consider, therefore, two expansions from a state of thermodynamic equilibrium of stagnation pressure p_o, enthalpy h_o and entropy s_o to a static pressure p. In the first expansion imagine the flow to remain throughout in complete thermodynamic equilibrium and denote the flow velocity and temperature at the end of the expansion by V_e and T_s respectively. T_s is, of course, the saturation temperature corresponding to the pressure p. In the second expansion, the flow, although remaining in inertial equilibrium (zero interphase velocity slip), is supposed to be completely frozen thermally, meaning that no phase change occurs. In this case let the exit velocity be V and the exit supercooling of the vapour phase be ΔT. In both cases the overall entropy remains constant and, as shown in the Appendix, to a very good approximation,

$$\left(\frac{V}{V_e}\right)^2 = 1 + \left[\frac{(1-y)c_p T_s}{V_e^2}\right]\left[\frac{\Delta T}{T_s}\right]^2 \tag{3}$$

where y is the exit wetness fraction in the nonequilibrium expansion and c_p is the isobaric specific heat capacity of the vapour phase.

In low pressure expansions, the supercooling is unlikely to rise above 35°C without triggering a strong nucleation, either primary or secondary. Considering an expansion to a flow velocity approximately equal to the sonic velocity, Eq (3) shows that the difference between V and V_e is unlikely to exceed 2%. Entropy increases brought about by real condensation effects will change this estimate slightly, but the order of magnitude remains the same. The conclusion is, therefore, that, unless the pressure distribution in a cascade is radically affected by nonequilibrium effects, the flow velocities will remain almost unchanged.

The Appendix also shows that the relationship between the steam densities at the end of the two hypothetical expansions is given, to a first approximation, by

$$\frac{\rho}{\rho_e} = 1 + \frac{\Delta T}{T_s}\left[\frac{1 - c_p T_s}{h_{fg}}\right] \tag{4}$$

where h_{fg} is the enthalpy of evaporation. Inserting typical values, it can be seen that the difference between ρ and ρ_e is unlikely to exceed 8%. Density changes due to nonequilibrium effects, although greater than velocity changes, are still unlikely to produce radical variations in the flow distribution.

The ρV product, which obviously has a direct influence on the mass flow coefficient via the continuity equation, may vary by up to 10% from the equilibrium

value. Should the mass flowrate rather than the pressure ratio be fixed, similar variations in pressure level might be expected. These depend strongly on Mach number, however, the pressure being notoriously sensitive to small changes in mass flowrate in the transonic regime.

Variations in exit flow angle are induced by thermal relaxation downstream of the cascade trailing edge as shown in Fig 1. These are quite different from, and should not be confused with, the deflection of a supersonic stream issuing from a blade passage and turning in the Prandtl–Meyer expansion fan centred on the trailing edge. Jet deflections caused by thermal relaxation occur both in subsonic and supersonic flow and can be estimated as follows. Assuming the pressure downstream of the blade row to remain constant, the momentum equation shows that the flow velocity is also constant. Simple application of the continuity equation then gives

$$\frac{\cos\beta}{\cos\beta_e}=\frac{\rho}{\rho_e} \tag{5}$$

where β is the flow angle measured from the axial direction. For turbine nozzle cascades with high outlet flow angles of around 70°, the maximum deviation (corresponding to $\rho/\rho_e=1.08$) is only 1.5°. On the other hand, for the flow emerging from a rotor row with a small absolute angle of swirl, the deviation may be 10–20°. This analysis is obviously inappropriate for near axial flows ($\beta_e\cong 0°$) and, in cases such as these, the streamsurfaces would rearrange themselves in the spanwise direction to accommodate the necessary increase in flow cross-sectional area.

As shown in the Appendix, the thermodynamic loss coefficient for the blade row can be approximated by

$$\zeta_T=\frac{2h_{fg}}{V_{ex}^2}\Delta y\left(\frac{\Delta T_{av}}{T_s}\right) \tag{6}$$

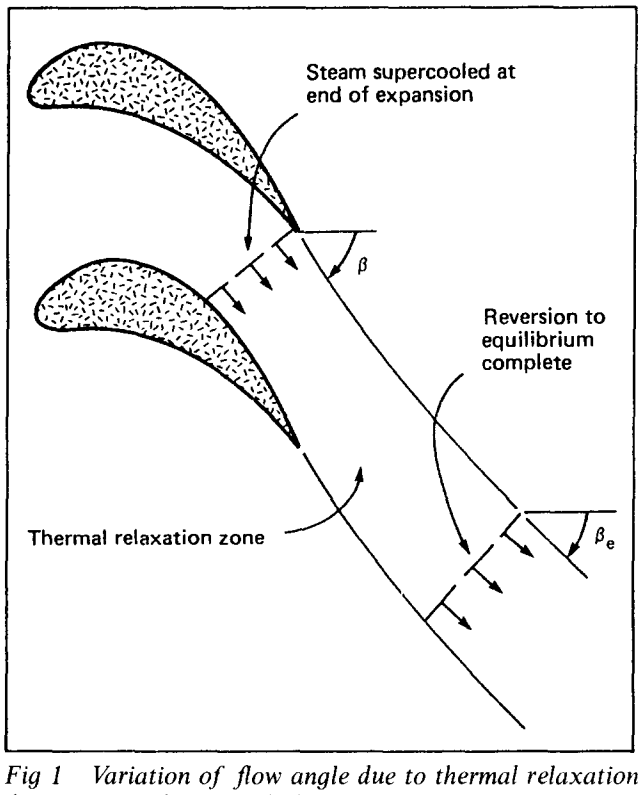

Fig 1 Variation of flow angle due to thermal relaxation downstream of a cascade (schematic)

where Δy is the increase in wetness fraction across the blade row and ΔT_{av} is a suitably defined mean supercooling. Insertion of typical values into Eq (6) shows that, under rather adverse conditions, ζ_T may approach values of the order of 0.1. Loss coefficients of such magnitude are obviously comparable to, or even greater than, the major aerodynamic sources of inefficiency.

These simple estimates, although of a very approximate nature, do give a good appreciation of the possible maximum effects of departures from thermal equilibrium. The following sections demonstrate how the various phenomena are affected by the local flow conditions and blade profiles and in particular show how deviations from equilibrium are reflected in the two-dimensionality of the flow patterns.

Examples of wet-steam flows in turbine cascades

Steam flowing through a turbine exists in different forms depending on its position within the machine. Assuming the condition line to have crossed the saturation line, the following categories can be identified:

(1) dry and supercooled throughout the blade passage;
(b) dry and supercooled at inlet, but a primary nucleation occurring within the blade passage;
(3) wet at inlet, but subsequently departing from equilibrium due to insufficient surface area for condensation on existing droplets;
(4) wet at inlet, but departures from equilibrium are so large that a secondary nucleation is induced in the blade passage.

The blade-to-blade time-marching computer program was used to calculate examples of the various flows described above. The blade profiles used for these studies were selected from Stages 4 and 6 of a six-stage low-pressure cylinder of an operational turbine-generator set. This turbine was also the subject of investigations by Yeoh[11], who performed a nonequilibrium axisymmetric throughflow calculation for the machine. The results of Yeoh's calculations were used in the present exercise for specifying the steam inlet conditions to the various blade passages.

Dry supercooled, non-nucleating flow

The throughflow calculations of Ref 11 suggested that the flow in the stator blade passages of Stage 4 is dry and supercooled despite the fact that the expansion is below the saturation line. Accordingly, the two-dimensional cascade program was used to investigate the influence of departures from equilibrium on the flow parameters in this regime.

Table 1 presents the input data and overall results for the root section of the blade. At inlet the steam is superheated by 15 K and the saturation line is crossed at about mid-chord. The equilibrium solution predicts a wetness of 1.5% at blade exit, but the nonequilibrium calculation shows that the steam is actually still dry and supercooled at this point, the nucleation rate (corresponding to $\Delta T=20°C$) being quite negligible. Departures from equilibrium are responsible for a 3% increase in mass flowrate (for the same pressure ratio), but the exit flow angle is unaffected. This is hardly surprising,

Table 1 Input data and results for root section of Stage 4 stator blade

p_o, bar	p_{ex}, bar	T_o, K	ΔT_{ex}, K	β_e°	β_{ne}°	ϕ	ξ_T
0.671	0.378	378	19	65.0	65.0	1.03	0.0

however, because the flow is subsonic and lossless throughout.

Fig 2 shows contours of constant supercooling from the nonequilibrium calculation, together with the blade surface pressure and velocity distributions. The velocities are normalized with respect to the frozen speed of sound at blade inlet. There is little difference between the pressure distributions from the two solutions, the maximum variation being about 3% on the suction surface. The variation in the velocity distributions is even smaller, in keeping with the order of magnitude predictions discussed previously.

Primary nucleating flows

Primary nucleating flows in turbines are of major importance because subsequent departures from equilibrium, the thermodynamic and other wetness losses are all strongly dependent on the fog droplet size. The throughflow calculations[11] demonstrated that the primary nucleation zone probably occurs in the rotor blade passage of Stage 4 and the blade-to-blade calculations were therefore carried out in order to investigate the effect of two-dimensionality on the process. A number of calculations were performed with different blade inlet temperatures in an attempt to model the fluctuations which occur in real turbines. The results are presented in Ref 9, to which the reader is referred for a detailed account. The general conclusions which emerged from the analysis were:

(a) The blade surface pressure and velocity distributions, and the exit flow angle were not greatly affected by nucleation.
(b) The thermodynamic loss coefficient was strongly dependent on the inlet temperature and, under adverse conditions, attained a value of 0.11.
(c) The mass flow coefficient varied between 1.0 and 1.06 depending on the position of nucleation.
(d) The mean fog droplet radius resulting from the primary nucleation was also dependent on the inlet stagnation conditions.

Wet, non-nucleating flows

Departures from equilibrium are not restricted to the primary nucleation zone, and the steam flowing in the succeeding stages may become supercooled if the rate of condensation on the droplet surface is insufficient to maintain the equilibrium demanded by the prevailing expansion rate. Just as with the primary nucleation, this also gives rise to a thermodynamic loss, although usually of a smaller magnitude. However, unlike the primary nucleation, which occupies only a small region of the turbine, non-nucleating wet-steam flows may prevail over several low pressure stages.

The steam entering Stage 6 of the 500 MW turbine is wet and at equilibrium according to the throughflow

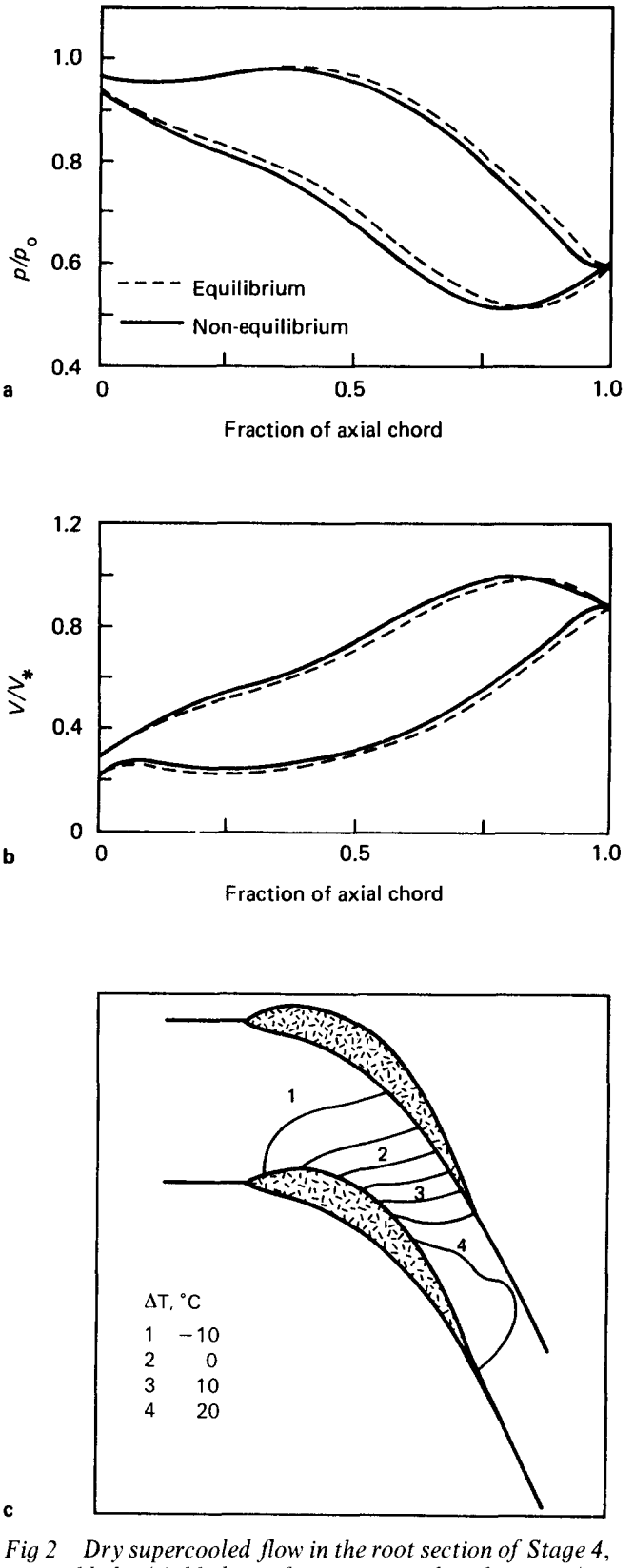

Fig 2 Dry supercooled flow in the root section of Stage 4, stator blade: (a) blade surface pressure distribution p/p_o; *(b) blade surface velocity distribution* V/V_*; *(c) contours of constant supercooling*

calculations, and the mid-height section of the stator blade was accordingly selected for analysis. The wetness fraction at inlet was obtained from the throughflow solution, but a range of different droplet radii were chosen in order to investigate the effect of droplet size on the

blade performance. Table 2 presents the input data and overall results.

A study of Table 2 reveals that there is no variation of outlet flow angle with droplet radius, nor is there any deviation from the equilibrium value. On the other hand, both the mass flow coefficient and the thermodynamic loss coefficient increase with droplet size.

Fig 3 shows the blade surface Mach number distribution based on the frozen speed of sound. It is notable that the equilibrium and various nonequilibrium solutions are virtually identical, despite the fact that the flow is transonic with an adiabatic shock wave situated near the trailing edge. Fig 3 also shows the variation of supercooling along the suction and pressure surfaces for three selected droplet radii of 0.05, 0.10 and 0.50 μm. With increasing droplet size, departures from equilibrium become more pronounced and this is reflected in an increase in supercooling, particularly on the suction surface. For the largest droplets ($r_o = 0.5$ μm) the supercooling rises sharply to 20°C near the trailing edge, but this is still insufficient to promote a secondary nucleation. In passing through the adiabatic shock wave, the vapour temperature rises, resulting in a decrease in supercooling and a return to equilibrium.

It is interesting to note that most of the thermodynamic loss occurs near the trailing edge of the blade where the supercooling is high. This is evident from the contours of constant entropy which are also shown in Fig 3 for the case of $r_o = 0.1$ μm. The explanation is that the thermodynamic entropy increase (which is associated with the interphase heat and mass transfer) is proportional to the square of the supercooling and this is only appreciable towards the end of the expansion.

Wet-steam flows with secondary nucleation

Secondary nucleations can occur in wet-steam flows when the expansion rate is high and the condensation rate on the existing droplets is insufficient to maintain the supercooling below the threshold for nucleation. The most

Table 2 Input data and results for mid-height section of Stage 6 stator blade

p_o, bar	p_{ex}, bar	T_o, K	r_o, μm	γ_o	β_e°	β_{ne}°	ϕ	ξ_T
0.16	0.07	327	0.01	0.055	72.0	72.0	1.000	0.005
0.16	0.07	327	0.05	0.055	72.0	72.0	1.007	0.006
0.16	0.07	327	0.10	0.055	72.0	72.0	1.014	0.010
0.16	0.07	327	0.30	0.055	72.0	72.0	1.022	0.019
0.16	0.07	327	0.50	0.055	72.0	72.0	1.032	0.027

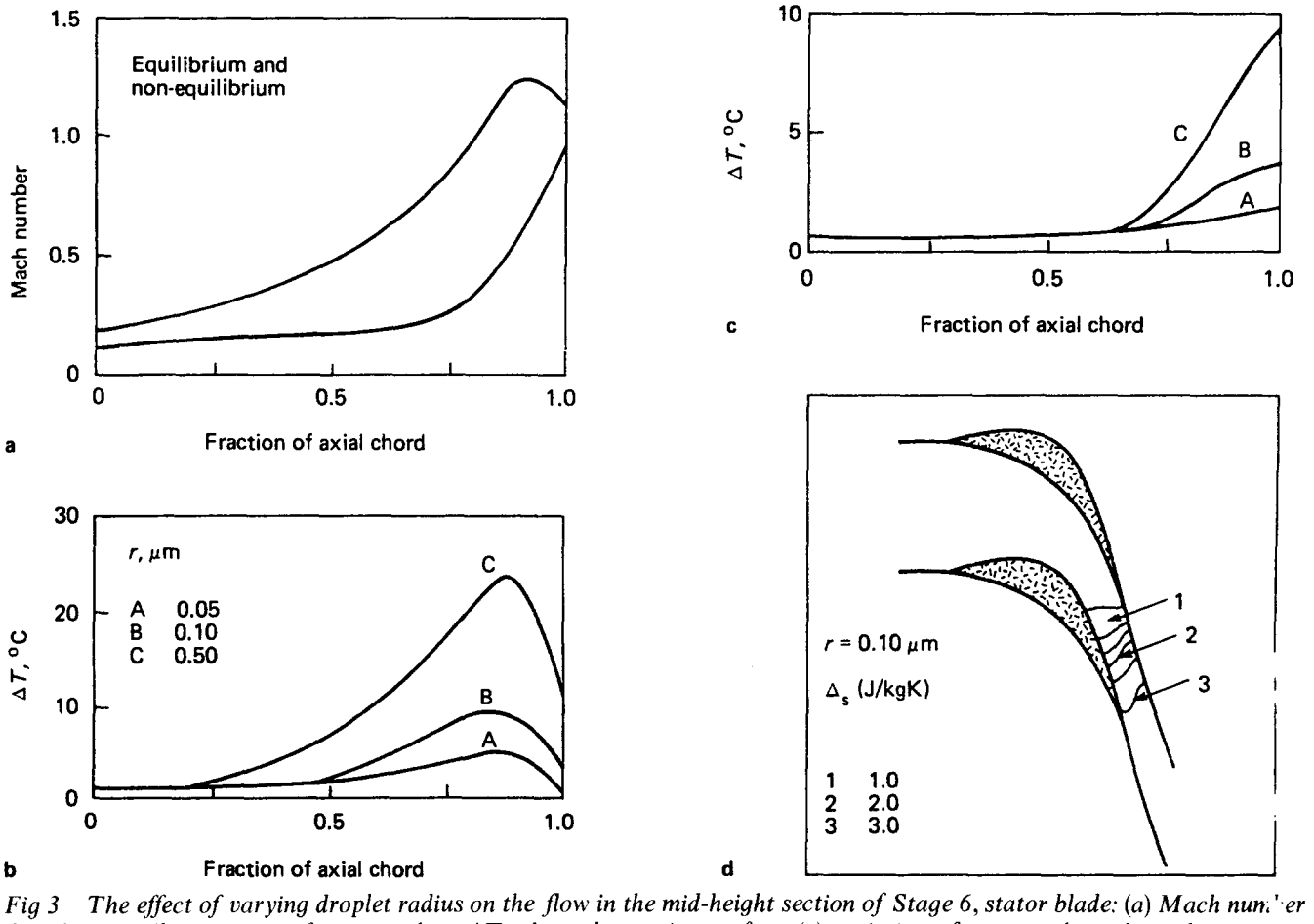

Fig 3 The effect of varying droplet radius on the flow in the mid-height section of Stage 6, stator blade: (a) Mach number distributions; (b) variation of supercooling, ΔT, along the suction surface; (c) variation of supercooling along the pressure surface; (d) contours of constant entropy rise

likely zones for secondary nucleations in large LP steam turbines are the root region of the stator blades and the tip region of the rotor blades of the final stage. The rotor tip and stator root sections of Stage 6 of the 500 MW turbine were therefore selected for analysis. The blade inlet and outlet conditions were obtained from the throughflow calculations, but the inlet primary droplet radii were chosen arbitrarily.

Table 3 shows the input data and overall results for the rotor tip section. A value of $r_o = 0.1$ μm was adopted for the inlet droplet radius, this being typical of the fog droplet size in LP turbines. However, despite the smallness of the primary droplets, the thermodynamic loss coefficient has a high value of 5.7%. It is also notable that the deviation of the exit flow angle due to nonequilibrium effects is only 1°, despite the high relative exit Mach number of 1.8.

In Fig 4 is shown the blade surface pressure distribution, which is again notable for the lack of distinction between equilibrium and nonequilibrium solutions. Also shown in the same figure are the contours of constant supercooling. It can be seen that the supercooling attains a value in excess of 25°C on the suction surface of the blade and this is sufficient to promote a weak secondary nucleation in this region.

When dealing with secondary nucleations, two separate droplet radii are retained in the calculations to represent the primary and secondary groups. This is thought to be a realistic theoretical model of the physical processes involved, but it should be appreciated that, as yet, no experimental evidence is available to justify the assumptions.

Fig 4 also shows the development of the primary and secondary droplet radii, together with the corresponding wetness fractions. Initially, due to the small wetness fraction associated with the secondary group, its thermal relaxation time is much larger than that of the primary group. The contribution of the secondary group to the overall relaxation time is therefore small and its presence makes little difference in the reversion to equi-

Table 3 Input data and results for Stage 6 rotor tip section

p_o, bar	p_{ex}, bar	T_o, K	r_o μm	y_o	β°_e	β°_{ne}	ϕ	ξ_T
0.154	0.044	327	0.1	0.07	56.5	57.5	1.01	0.057

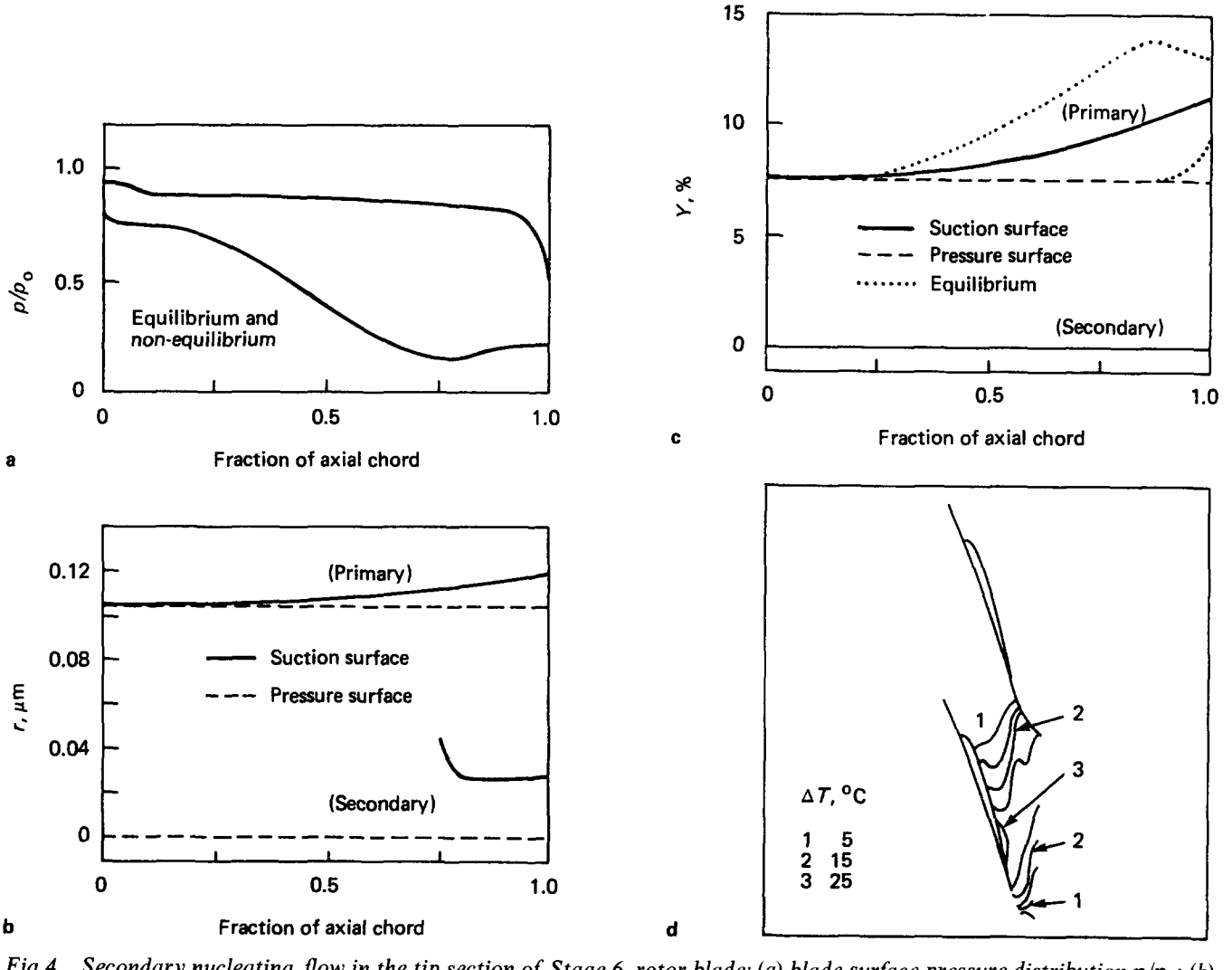

Fig 4 Secondary nucleating flow in the tip section of Stage 6, rotor blade: (a) blade surface pressure distribution p/p_o*; (b) droplet radius* r*; (c) wetness* y*; (d) contours of constant supercooling*

Table 4 Input data and results for root section of Stage 6 stator blade

p_o, bar	p_{ex}, bar	T_o K	r_o μm	y_o	β_e°	β_{ne}°	ϕ	ζ_T
0.160	0.026	327	0.5	0.055	47.0	48.0	1.01	0.088

librium occurring downstream of the trailing edge. The majority of the water present and the effective surface area for condensation is largely due to the primary droplet group.

In passing, it is worth noting that the tip section of a final stage rotor blade presents one of the most difficult computational problems for any blade-to-blade calculation technique. The fact that the computer program can deal, not only with the difficult geometry, but also with the secondary nucleation, demonstrates more than anything else its 'numerical robustness'.

The second calculation of secondary nucleation presented here is for the root section of the stator blade of Stage 6. The input data and overall results appear in Table 4. The primary droplet radius was chosen to be 0.5 μm in order to demonstrate the rather different results obtaining when a secondary nucleation occurs in the presence of large droplets.

The flow through this section of the blade passage is supersonic with an adiabatic oblique shock wave. The contours of constant supercooling in Fig 5 show that the expansion rate is high, resulting in a degree of supercooling greater than 30°C near the blade trailing edge. A secondary droplet group therefore forms near the suction surface. The droplets are very small with a mean radius of 0.01 μm, but they are present in such large numbers that their relaxation time is comparable to that of the primary group. The secondary group therefore presents a large surface area for condensation and plays a major part in the reversion to equilibrium. This can be seen from the graphs of droplet radius and wetness fraction also shown in Fig 5.

Conclusions

The following conclusions are based on the calculations reported in the previous sections. It should be appreciated, however, that as yet there are no experimental data available either to confirm or refute the findings.

(1) *For a prescribed cascade pressure ratio*, the variations in blade surface pressure and velocity distributions due to departures from thermal equilibrium are small (< 5%). In those examples computed to date, there is no evidence of radical changes in flow distribution due to nonequilibrium condensation. From this point of view, therefore, the added complexity and sophistication of nonequilibrium blade-to-blade calculations is only necessary in cases where extreme accuracy is required.

(2) The variation in blade exit relative flow angle due to thermal relaxation is at most 1°–2° and is usually less.

(3) The tendency for the mass flowrate to increase with departures from equilibrium is significant, and mass flow coefficients should be included in performance calculation methods. Usually $1.0 < \phi < 1.06$.

(4) The thermodynamic loss is a major component of the overall loss in the final stages of LP turbines. ζ_T is a

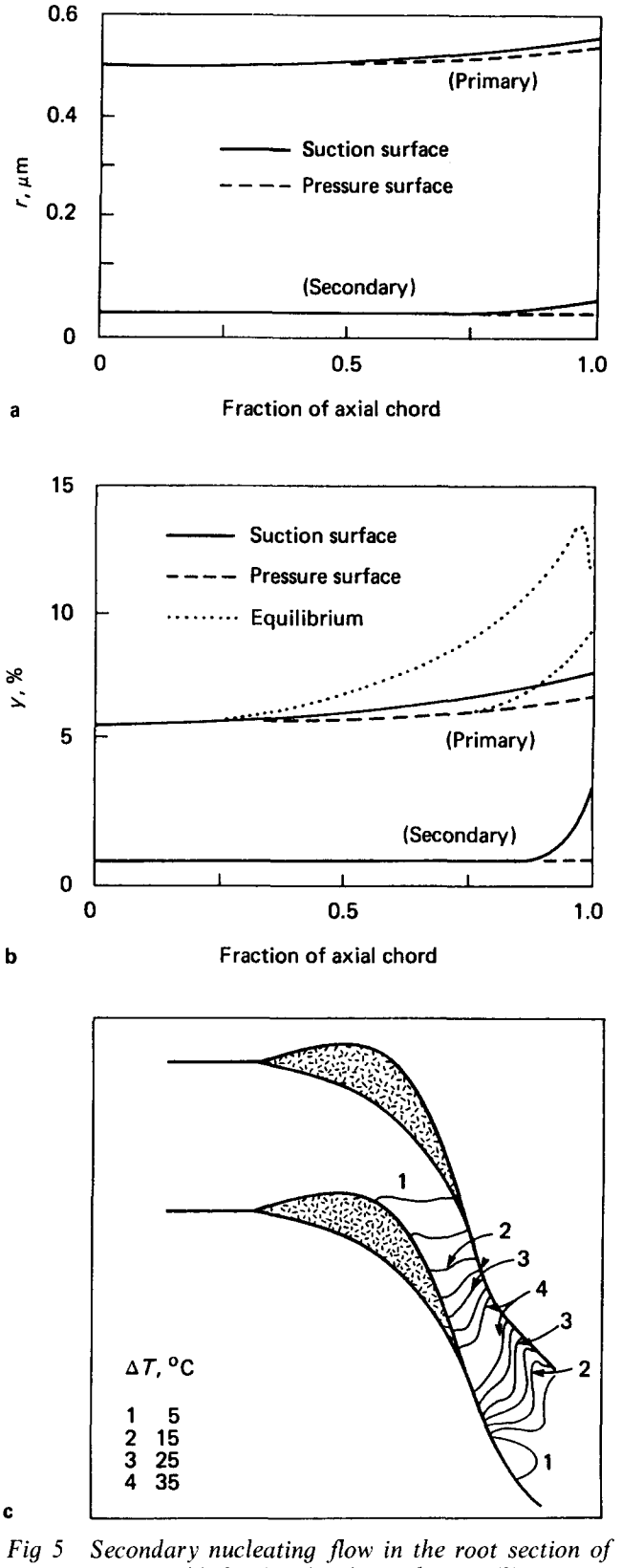

Fig 5 Secondary nucleating flow in the root section of Stage 6, stator blade: (a) droplet radius r; (b) wetness y;(c) contours of constant supercooling

strong function of the droplet radius and the local flow conditions and, in general, $0.0 < \xi_T < 0.11$. The Baumann rule, which correlates the wetness loss with the wetness fraction rather than the droplet size, is unsatisfactory.

(5) The mean radius of primary fog droplets is very sensitive to the local conditions at the Wilson Point, and strong circumferential variations in droplet radius may occur under certain conditions. Because of this sensitivity (and also because of the inability of present methods to determine the contribution to the droplet population from nucleation in blade wakes and due to mainstream turbulence), a reliable procedure for predicting the mean fog droplet radius in turbines is unlikely to be forthcoming in the foreseeable future.

(6) Secondary nucleations are likely to occur at the stator root and rotor tip regions of the final stage and generally give rise to high thermodynamic loss. These might be avoided by judicious design of blade profiles.

Acknowledgements

The authors gratefully acknowledge the assistance given by the staff of the Mechanical Research Department, NEI Parsons Ltd. One of the authors (MM) was supported by an SERC studentship during the course of the work at the Whittle Laboratory, University of Cambridge.

References

1. **Miller E. H. and Schofield P.** The performance of large steam turbine generators with water reactors. *ASME Winter Annual Meeting, New York, Nov 1972*
2. **Baumann K.** Some recent developments in large steam turbine practice. *Engineering, 1921,* **3**
3. **Gyarmathy G.** Bases of a theory for wet steam turbines. *Bulletin 6, Inst. for Thermal Turbomachines, Federal Technical University, Zurich, 1962*
4. **Yeoh C. C. and Young J. B.** Non-equilibrium streamline curvature throughflow calculations in wet steam turbines. *Trans. ASME, J. Engng. for Power, 1982,* **104**, *489*
5. **Yeoh C. C. and Young J. B.** Non-equilibrium throughflow analyses of low pressure wet steam turbines. *Trans. ASME, J. Engng. for Power, 1984,* **106**, *716*
6. **Bakhtar F. and Tochai M. T. M.** An investigation of two-dimensional flows of nucleating and wet steam by the time-marching method. *Int. J. Heat and Fluid Flow, 1980,* **2**, *5*
7. **Snoeck J.** Two-dimensional condensing flow in transonic turbine cascades. *VKI Lecture Series 1983—06. Aerothermodynamics of Low Pressure Steam Turbines and Condensers, 1983*
8. **Bakhtar F. and Alubaidy A. K.** On the solution of supersonic blade-to-blade flows of nucleating steam by the time-marching method. *Inst. Mech. Engnrs., Conference on 'Computational Methods in Turbomachinery', University of Birmingham, 1984, Paper C82/84, 101*
9. **Moheban M. and Young J. B.** A time-marching method for the calculation of blade-to-blade non-equilibrium wet steam flows in turbine cascades. *Inst. Mech. Engnrs., Conference on 'Computational Methods in Turbomachinery', University of Birmingham, 1984, Paper C76/84, 89*
10. **Denton J. D.** An improved time-marching method for turbomachinery flow calculation. *Trans. ASME, J. Engng. for Power, 1983,* **105**, *514*
11. **Yeoh C. C.** Non-equilibrium throughflow calculations in steam turbines. *PhD Thesis, Cambridge University Engineering Department, 1981*

Appendix

Departures from thermal equilibrium

Consider an expansion of wet steam from stagnation enthalpy h_o and entropy s_o such that the flow remains in thermodynamic equilibrium. Assuming adiabatic flow, the steady flow energy equation can be written

$$h_o = (1-y_e)h_{ge} + y_e h_{le} + \frac{V_e^2}{2} \tag{A1}$$

Now consider a thermally frozen expansion from the same inlet stagnation conditions to the same static pressure p. Assuming zero phase change and zero interphase velocity slip, the steady flow energy equation becomes

$$h_o = (1-y)h_g + y h_l + \frac{V^2}{2} \tag{A2}$$

Assuming the vapour phase to behave as a perfect gas,

$$h_g = h_{ge} - c_p \Delta T \tag{A3}$$

where ΔT is the supercooling developed at the end of the nonequilibrium expansion. Also, neglecting the capillary supercooling of the droplets,

$$h_l = h_{le} \tag{A4}$$

Combining equations (A1) to (A4) gives

$$\frac{V^2 - V_e^2}{2} = (y - y_e)h_{fg} + (1-y)c_p \Delta T \tag{A5}$$

where $h_{fg} = h_{ge} - h_{le}$ is the enthalpy of evaporation.

The entropy is constant in both expansions, and so

$$s_o = (1-y_e)s_{ge} + y_e s_{le} = (1-y)s_g + y s_l \tag{A6}$$

Noting that $s_l = s_{le}$ and

$$s_{ge} - s_g = -c_p \ln(1 - \Delta T/T_s) \tag{A7}$$

where T_s is the saturation temperature corresponding to the pressure p, gives

$$(y - y_e)(s_{ge} - s_{le}) = (1-y)c_p \ln(1 - \Delta T/T_s) \tag{A8}$$

Combination of Eqs (A5) and (A8) together with expansion of the logarithmic term, then leads to

$$\left(\frac{V}{V_e}\right)^2 = 1 + \left[\frac{(1-y)c_p T_s}{V_e^2}\right]\left[\frac{\Delta T}{T_s}\right]^2 \tag{A9}$$

Considering now the ratio of the densities for the two expansions (and assuming the vapour phases to behave as perfect gases),

$$\frac{\rho}{\rho_e} = \frac{\rho_g}{\rho_{ge}}\left[\frac{1-y_e}{1-y}\right] = \frac{T_s}{T_g}\left[\frac{1-y_e}{1-y}\right] \tag{A10}$$

Introducing Eq (A8)

$$\frac{\rho}{\rho_e} = \left[\frac{1}{1 - \Delta T/T_s}\right]\left[1 + \frac{c_p T_s}{h_{fg}}(1 - \Delta T/T_s)\right] \tag{A11}$$

Hence, to a first approximation,

$$\frac{\rho}{\rho_e} \cong 1 + \frac{T}{T_s}\left(1 - \frac{c_p T_s}{h_{fg}}\right) \tag{A12}$$

As shown in Ref 9, the thermodynamic entropy increase is given by

$$\frac{ds_T}{dt} \cong h_{fg} \frac{\Delta T}{T_s^2} \frac{dy}{dt} \quad \text{(A13)}$$

Across a blade row,

$$\Delta s_T = h_{fg} \frac{\Delta T_{av}}{T_s^2} \Delta y \quad \text{(A14)}$$

where Δy is the increase in wetness fraction and ΔT_{av} is a suitably defined average value of the vapour supercooling. Substituting Eq (A14) into Eq (2) gives

$$\xi_T = \frac{2h_{fg}}{V_{ex}^2} \Delta y \left(\frac{\Delta T_{av}}{T_s} \right) \quad \text{(A15)}$$

CALENDAR

Direct and Large Eddy Simulation of Turbulent Flows (Euromech. colloquium)	30 September–1 October 1985 Munich, FRG	Professor R. Friedrich, Lehrstuhl für Stromungsmechanik, Technische University München, Acisstrasse 21, 8000 München 2, FRG
Measurement Techniques in Low-speed Turbulent Flows (Euromech. colloquium)	7–9 October 1985 Marknesse, The Netherlands	Dr B. van den Berg, National Aerospace Laboratory NLR, Voorsterweg 31, 8316 PR Marknesse, The Netherlands
Industrial Heat Exchanger Technology Symposium	6–8 November 1985 Pittsburgh, PA, USA	Conferences and Expositions, American Society for Metals, Metals Park, OH 44073, USA
ASME Winter Annual Meeting	17–21 November 1985 Miami, FL, USA	ASME, 345 East 47th Street, New York, NY 10017, USA
Fluid Transients in Fluid Structure Interaction – 2nd Symposium	17–21 November 1985 Miami, FL, USA	ASME, 345 East 47th Street, New York, NY 10017, USA
Fundamental Aspects of Gas Liquid Flows	17–21 November 1985 Miami, FL, USA	Professor E. E. Michaelides, Mechanical and Aerospace Engineering, University of Delaware, Newark, DE 19716, USA
Numerical Methods for Multiphase Flow (course)	18–22 November 1985 Ispra, Italy	Secretariat 'Ispra-Courses', Centro Commune di Ricerca, I-21020 Ispra (Varese), Italy
AIAA Joint Fluid Dynamics and Heat Transfer Conference	12–14 May 1986 Atlanta, GA, USA	American Institute of Aeronautics and Astronautics, 1290 Avenue of the America, New York, NY 10019, USA
Water for Energy	14–16 May 1986 Brighton, UK	BHRA Fluid Engineering Centre, Cranfield, Bedford MK43 0AJ, UK
31st International Gas Turbine Conference and Exhibit	8–12 June 1986 Dusseldorf, FRG	ASME, 345 E. 47th Street, New York, NY 10017, USA
Flow Measurement in the Mid-80s	9–12 June 1986 Glasgow, UK	Conference Section, National Engineering Laboratory, East Kilbride, Glasgow G75 0QU, UK
6th International Symposium: Finite Element Methods in Flow Problems	16–20 June 1986 Antibes, France	INRIA, Service des Relations Extérieures Rocquencourt, BP 105, 78153 Le Chesnay Cedex, France
8th International Heat Transfer Conference	17–22 August 1986 San Francisco, CA, USA	Chang-Lin Tien, Department of Mechanical Engineering, University of California, Berkeley, CA 94720, USA
7th International Fluid Power Symposium	16–18 September 1986 Bath, UK	BHRA, The Fluid Engineering Centre, Cranfield, Bedford MK43 OAL, UK
5th International Conference on Pressure Surges	22–24 September 1986 Hannover, FRG	BHRA Fluid Engineering Centre, Cranfield, Bedford MK43 0AJ, UK
ASME Winter Annual Meeting: International Symposium on Pressure and Temperature Measurement	30 November–5 December 1986 San Francisco, CA, USA	Dr J. H. Kim, Electric Power Research Institute, 3412 Hillview Avenue, PO Box 10412, Palo Alto, CA 94303, USA
Australian Fluid Mechanics Conference	8–12 December 1986 Auckland, New Zealand	AFMC Conference Committee, c/o Dr P. S. Jackson, Dept of Mechanical Engineering, Auckland University, Private Bag, Auckland, New Zealand